IOSR Journal of Mechanical and Civil Engineering (IOSR-JMCE)
e-ISSN: 2278-1684,p-ISSN: 2320-334X, Volume 13, Issue 4 Ver. II (Jul. - Aug. 2016), PP 18-24
www.iosrjournals.org

CFD Analysis ofWind Turbine Airfoil at Various Angles of Attack

Ankan Dash
(School of Mechanical Engineering, KIIT University, India)

Abstract: *The main aim of the study was to analyze the NACA0012 wind turbine airfoil at various angles of attack, keeping the Reynolds number constant. The efficiency of the aerodynamic wind turbine is greatly influenced by the aerodynamic efficiency of the airfoil. In the present study NACA0012 airfoil is considered as a suitable wind turbine blade. The geometry and analysis was done using Ansys-Fluent. Calculations were done for constant air velocity altering only the angle of attack. For the computational domain an unstructured mesh with sphere of influence and inflation was selected, taking care of the refinement of the grid near the airfoil in order to enclose the boundary layer approach. The CFD simulation results show close agreement with the results obtained from wind tunnel testing experiments, thus suggesting CFD analysis as a reliable alternative to experimental methods.*

Keywords: *Airfoil, Angle of Attack, CFD, Drag Coefficient,Lift Coefficient*

I. Introduction

Airfoil is defined as the cross-section of a body that is placed in an airstream in order to generate useful aerodynamic force. Compressor and turbine blades, wings of aircraft, propeller blades, windmill blades and hydrofoils are all examples of airfoils. The shape of an airfoil blade is one of the most critical partof a wind turbine, as the blade is responsible for the conversion of kinetic energy to mechanical energy.Computational Fluid Dynamics (CFD) is a branch of fluid mechanics that uses numerical methods and algorithms to solve complex problems involving fluid flow. Some of the recent interesting work in the study of airfoils has been discussed below. Patil et al. [1] investigated the effect of low Reynolds number on lift and drag for the wind turbine blade. They found out as Reynolds number increases, lift and drag forces increases.Haque et al. [2] conducted various experimental studies to understand the effects of Reynolds number and angle of attack in flow analysis. Yao et al. [3] studied the aerodynamic performance of wind turbine airfoils and compared the numerical results with experimental data. The effect of transonic flow over an airfoil has been studied and a comparative analysis hasbeen done to analyze the variation of angle of attack and Mach number [4]. The comparison of various turbulence models (Spalart-Allmaras, Realizable $k-\varepsilon$ and $k-\omega$ shear stress transport) has been done and it was found out that the turbulence models used in commercial CFD codes does not give accurate results yet at high angle of attack [5]. The mechanism of laminar separation bubble and laminar-turbulent separation over the airfoil has been analyzed by Shah et al. [6] and the relationship between angle of attack and laminar bubble separation, Reynolds number and laminar bubble separation was studied. The analysis of stall angle and its effects on lift and drag coefficient was reported by Sahin et al. [7].

In the light of the review of the existing literature, the present study aims to analyze the flow field for NACA 0012 wind turbine airfoil at various angles of attack with constant Reynolds number of 10^6. The flow was obtained by solving the steady-state governing equations of continuity and momentum conservation with Realizable $k-\varepsilon$ turbulence model and the results were validated by comparing with the available experimental data.

Lift Coefficient (C_L): It is a dimensionless quantity that relates the lift generated by airfoil to the fluid density around the body, the fluid velocity and an associated reference area.

$$C_L = \frac{L}{\frac{1}{2}\rho v^2 A} \tag{1}$$

Where,
L is the lift force,
ρ is the density of air,
V is inlet velocity of air,
A is the area of airfoil.

Drag Coefficient (C_D): It is a dimensional quantity that is used to quantify the drag or resistance of an object in a fluid environment.

$$C_D = \frac{D}{\frac{1}{2}\rho v^2 A} \tag{2}$$

Where,
D is the drag force,
ρ is the density of air,
V is inlet velocity of air,
A is the area of airfoil.

II. Geometry And Mesh Generation

For discretization of the computational domain, an unstructured mesh with sphere of influence centered on the middle of the airfoil was selected. The mesh used for the analysis is shown in the Fig.2. Pressure based steady state solver with Realizable $k - \varepsilon$ turbulence model is used for analysis.

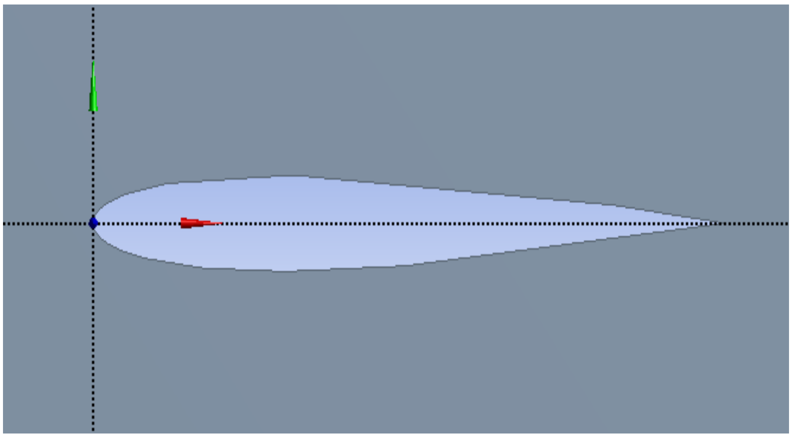

Figure 1. Geometry of NACA 0012 Airfoil

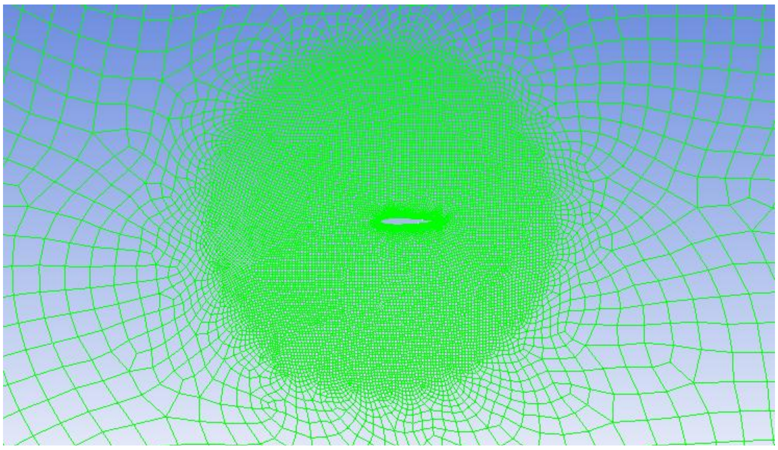

Figure 2. Mesh of the computational domain

III. Inputs and Boundary conditions

The problem consists of flow around an airfoil at various angles of attack (4, 6, 8, 10 degree). The inputs and boundary conditions are shown in the Table below.

Table 1 Inputs and boundary conditions

No	Input	Value
1	Fluid medium	Air
2	Velocity of flow	51.4496 m/s
3	Operating pressure	101325 Pa
4	Density of fluid	1.1767 kg/m^3
5	Reynolds number	10^6
6	Chord length	1 m
7	Operating temperature	277 k
8	Angles of attack	4, 6, 8, 10 degree
9	Model	Realizable $k - \varepsilon$
10	Viscosity	1.009×10^{-5} kg/m.s

IV. Results And Discussion

4.1 Contours of velocity magnitude

The contours of velocity magnitude obtained for various angles of attack from CFD simulations are shown in the following Fig. 3, 4, 5 and 6. On the leading edge, we can see the stagnation point where the velocity of flow is nearly zero. The fluid accelerates on the upper surface of the airfoil while the velocity of the fluid decreases along the lower surface of the airfoil.

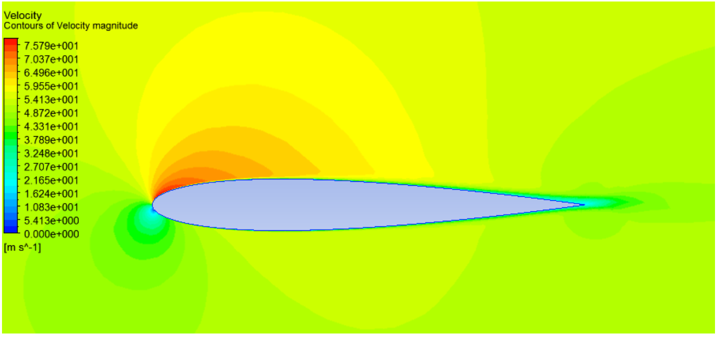

Figure 3. Contours of velocity magnitude at 4 degree of angle of attack

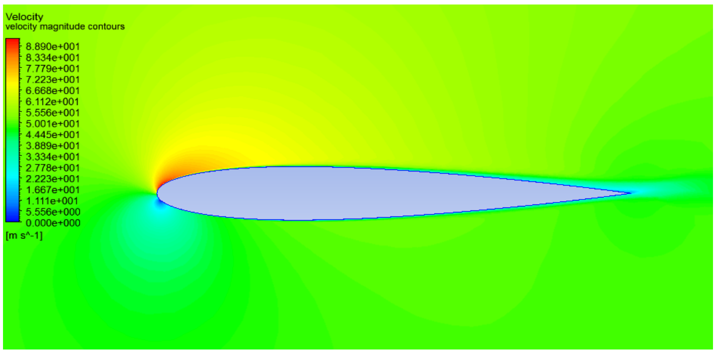

Figure 4. Contours of velocity magnitude at 6 degree of angle of attack

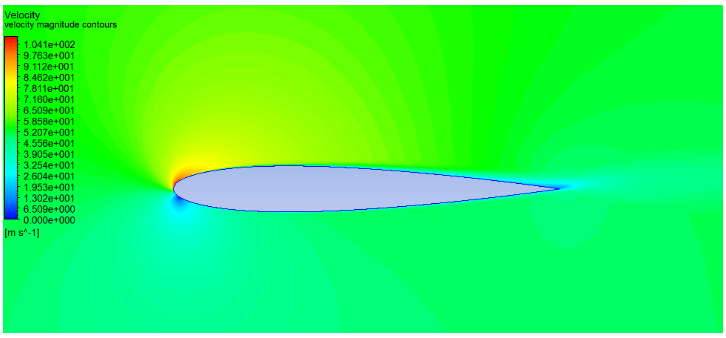

Figure 5. Contours of velocity magnitude at 8 degree of angle of attack

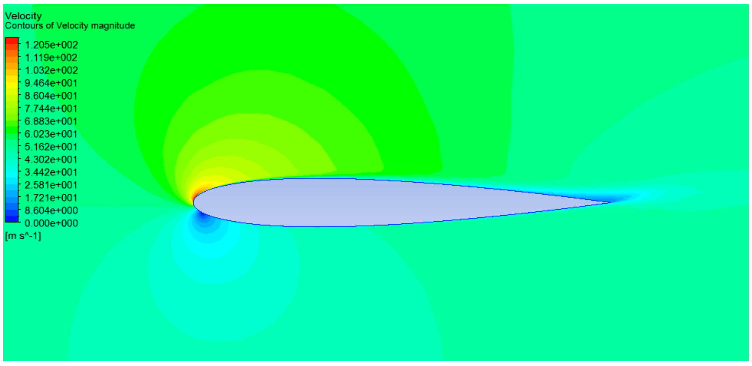

Figure 6. Contours of velocity magnitude at 10 degree of angle of attack

4.2 Contours of pressure magnitude

The contours of pressure magnitude obtained for various angles of attack from CFD simulations are shown in the following Fig.7, 8, 9and 10. We can see the flow accelerates on the upper side of the airfoil and the velocity of flow decreases along the lower side, according to Bernoulli's principle the upper surface will experience low pressure and the lower surface will experience higher pressure. Hence the value of lift coefficient will increase and the value of drag coefficient will also increase but the increase in drag is low in comparison to the increase in lift force.As the pressure on the lower surface of the airfoil is greater than that of the incoming flow stream, the airfoil is effectively pushed upward normal to the incoming flow stream.

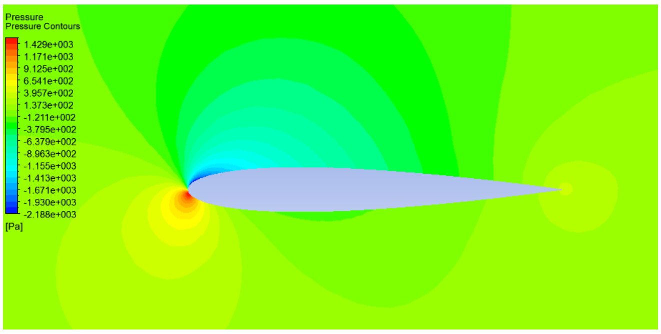

Figure 7. Pressure contours at 4 degree of angle of attack

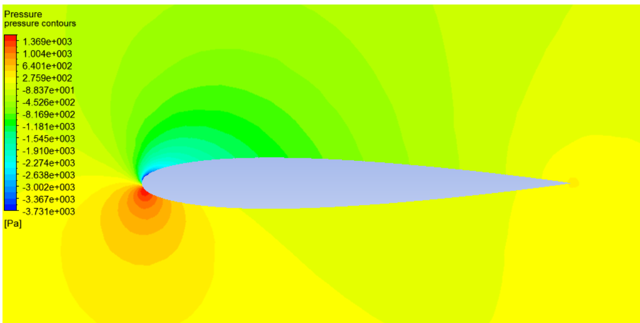

Figure 8. Pressure contours at 6 degree of angle of attack

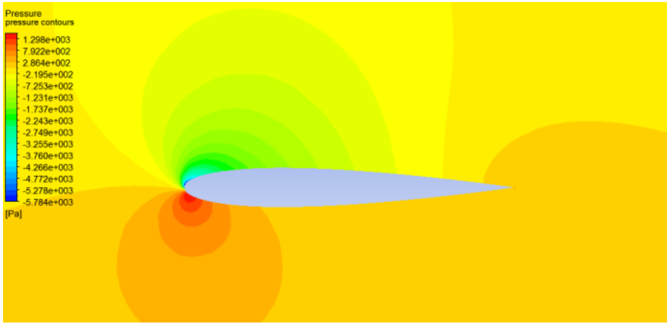

Figure 9. Pressure contours at 8 degree of angle of attack

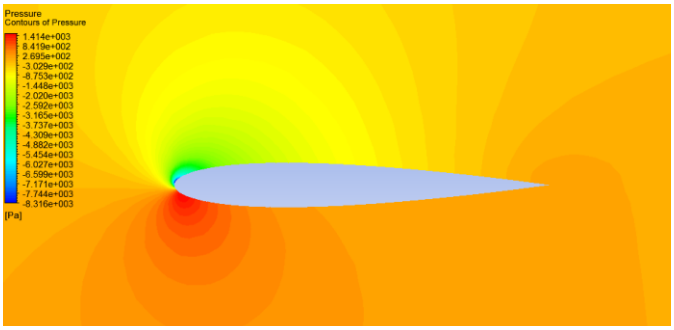

Figure 10. Pressure contours at 10 degree of angle of attack

4.3 Distribution of pressure coefficient

The distribution of pressure coefficient of NACA0012 airfoil under different angles of attack is shown in the following Fig. 11, 12, 13, and 14. It can be seen that the pressure coefficient varied largely under different attack angle. The pressure coefficient of the airfoil's upper surface was negative and the lower surface was positive, thus the lift force of the airfoil is in the upward direction. Larger the attack angle, greater is the difference of pressure coefficient between the lower and upper surface. We can also see that the coefficient of pressure difference is much larger on the front edge, while on the rear edge it was much lower, thus indicting that the lift force of the airfoil is mainly generated from the front edge.

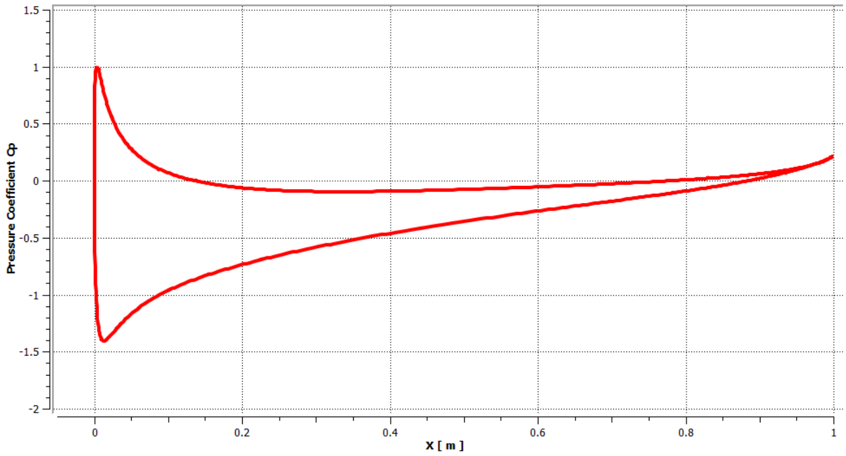

Figure 11. Pressure coefficient at 4 degree angle of attack

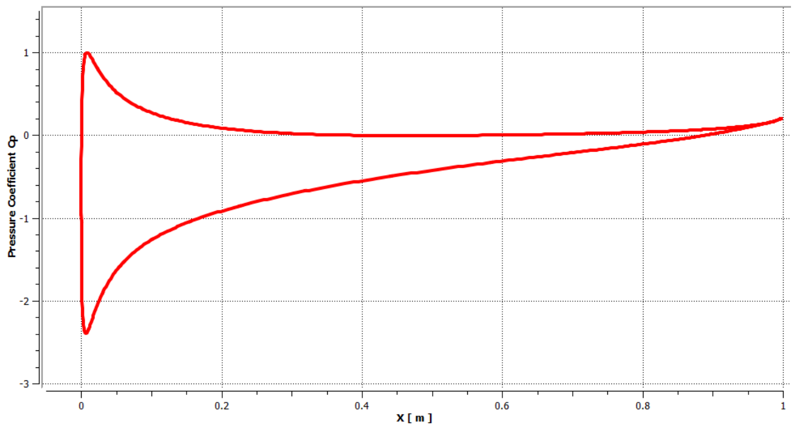

Figure 12. Pressure coefficient at 6 degree angle of attack

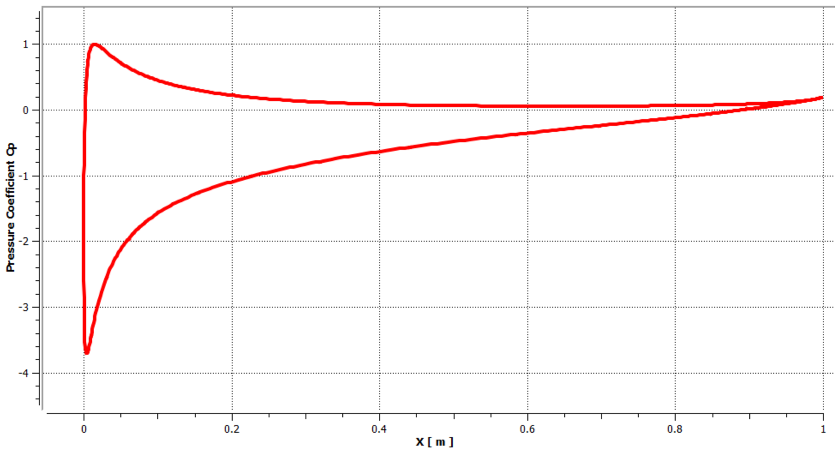

Figure 13. Pressure coefficient at 8 degree angle of attack

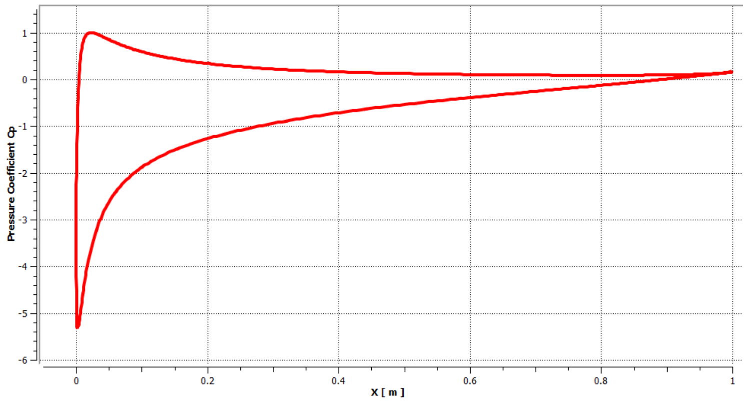

Figure 14. Pressure coefficient at 10 degree angle of attack

4.4 Curves of lift and drag coefficient

The curves of lift and drag coefficient are computed at various angles of attack using the Realizable $k - \varepsilon$ turbulence model. The results of the CFD simulation were compared with the experimental results and were validated with the existing literature for NACA0012 airfoil, which indicate a good correlation between the results obtained from CFD analysis and the results obtained through experiments.

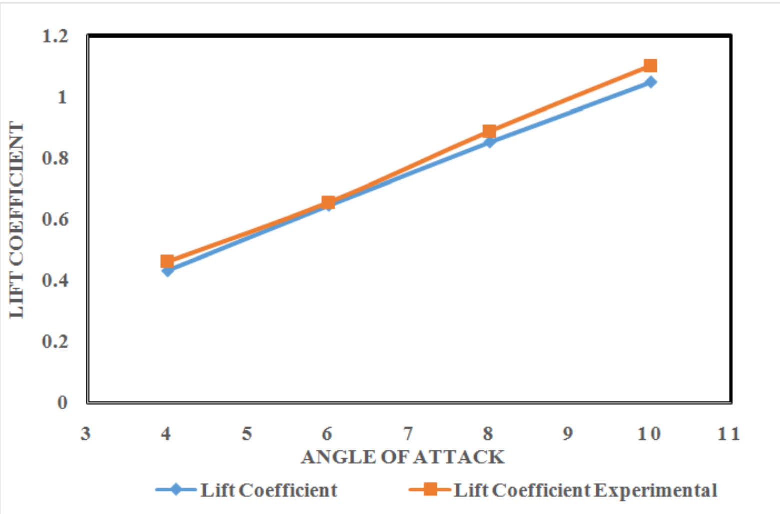

Figure 15. Graph of Lift Coefficient vs. Angle of Attack

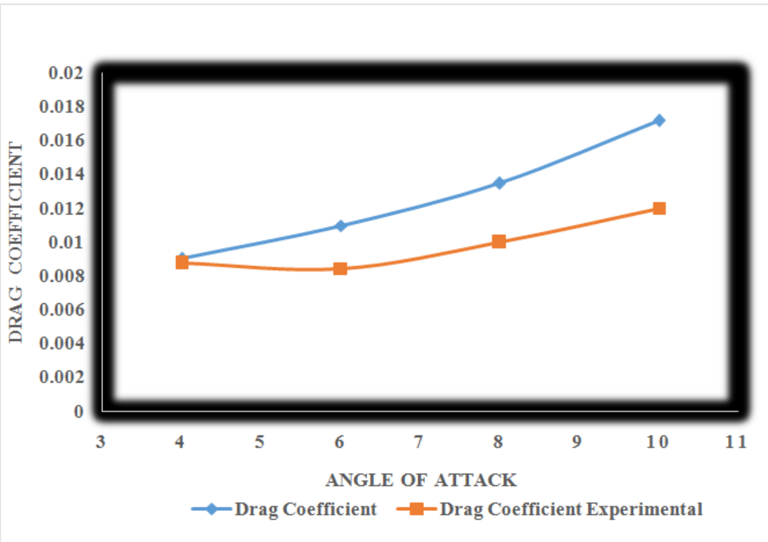

Figure 16. Graph of Drag Coefficient vs. Angle of Attack

V. Conclusion

With the help of CFD software Ansys-Fluent, successful analysis of aerodynamic performance of NACA0012 airfoil has been carried at various angles of attack (4, 6, 8, 10 degree) with constant Reynolds number (10^6)using the Realizable$k - \varepsilon$turbulence model. It is seen that the velocity of upper surface is higher than the velocity of the lower surface. The pressure coefficient of the airfoil's upper surface was negative and the lower surface was positive, thus the lift force of the airfoil is in the upward direction. The coefficient of pressure difference is much larger on the front edge, while on the rear edge it was much lower. It is observed that to increase the value of lift force and lift coefficient we have to increase the value of angle of attack. This leads to rise in drag force and drag coefficient as well, but the increase in drag force and drag coefficient is quite low in comparison to lift force and lift coefficient. Computed drag and lift forces were found in close agreement with the experimental values thus corroborating that CFD analysis is an efficient alternative to experimental methods.

Acknowledgements

I would like to sincerely express my deep gratitude to KIIT School of Mechanical Engineering for providing me an opportunity and necessary facilities to carryout this work.

References

[1] Bhushan S. Patil, Hitesh R. Thakare, Computational Fluid Dynamics Analysis of Wind Turbine Blade at Various Angles of Attack and different Reynolds Number, *Procedia Engineering, 127(2015),* 1363-1369

[2] NazmulHaque, Mohammad Ali, IsmatAra, Experimental Investigation on the performance of NACA 4412 aerofoil with curved leding edge planform, *Procedia Engineering, 105(2015)*, 232-240

[3] Jin Yao, Weibin Yuan, Jianliang Wang, JianbinXie, Haipeng Zhou, MingjunPeng, yong Sun, Numerical simulation of aerodynamic performance for two dimensional wind turbine airfoils, *Procedia Engineering, 31(2012),* 80-86

[4] Novel Kumar Sahu, Mr. Shadab Imam, Analysis of Transonic Flow over an Airfoil NACA0012 using CFD, *International Journal of Innovative Science, Engineering & Technology, Vol. 2 Issue 4,* April 2015

[5] Douvi C. Eleni, Tsavalos I. Athanasios, Margaris P Dionissios, Evaluation of the turbulence models for the simulation of the flow over a National Advisiory Committee for Aeronautics (NACA) 0012 airfoil, *Journal of Mechanical Engineering Research, Vol.4(3),pp.* 100-111 March 2012

[6] Haseeb Shah, Sathyajith Mathew, Chee Ming Lim, Numerical simulation of flow over an airfoil for small wind turbines using the $\gamma - Re_\theta$ model, *The International Journal of Energy and Environmental Engineering, (2015) 6:* 419-429

[7] IzzetSahin, AdemAcir, Numerical and Experimental Investigations of Lift and Drag Performances of NACA 0015Wind Turbine Airfoil, *International Journal of Materials, Mechanics and Manufacturing, Vol. 3, No. 1,* February 2015

[8] S. Khandwal, S. Singh, Computational fluid dynamics study of fluid flow and aerodynamic forces on an airfoil, *International Journal of Engineering Research and Technology, 2012 vol. 1, Issue. 7*

[9] A. Prabhakar, A CFD analysis of static and dynamic pressure for NACA4412, *International Journal of Engineering Trends and Technology, 2013, vol. 4issue 8,* pp. 3258-65